Influence of strain-induced crystallization on the crack driving force in fracture behavior of rubber

Joachim Guilie, Patrick Le Tallec

YIC2013
Second ECCOMAS Young Investigators Conference
2–6 September 2013, Bordeaux, France

Influence of strain-induced crystallization on the crack driving force in fracture behavior of rubber

J. Guilie [a,*], P. Le Tallec [a]

[a] LMS
Ecole Polytechnique, 91128 Palaiseau, France

*joachim.guilie@gmail.com

Abstract. *Fatigue crack growth resistance increases with the loading ratio due to strain-induced crystallization, even if the peak stress increases. Recent experiments have allowed determination of the strain-induced crystallization (SIC) distribution around a crack tip during uninterrupted fatigue tests. The purpose of this work is to compare spatial distributions of crystallinity in a cracked sample at different elongations between one experiment and simulation results based on our model.*

Keywords: Crack; Strain-induced crystallization; Micro-sphere.

The study of fatigue crack propagation in elastomers is of major importance for the tyre industry; the goal is to improve the service life of products. Vulcanized cis-1,4-polyisoprene (natural rubber; NR) is a key compound in tyres; it exhibits remarkable mechanical properties and more particularly a very good resistance to fatigue crack growth as compared with synthetic rubbers, especially for large strain. It is widely recognized that these excellent fatigue properties are related to the ability of NR to crystallize under strain (Beurrot 2012). In that framework, our objective is to compare the experimentally determined crystallization distribution around a crack tip in a pure-shear sample during uninterrupted fatigue tests (Rublon 2012) and the results given by our model (Guilie 2013a). We therefore first review in section 1 state-of-the-art experiments and identify a recent experiment on a cracked sample, which, we think, is ideal for comparisons with our model. We then construct a constitutive law in section 2 from an adequate choice of free energy and internal variables. The model is then validated on a cracked sampled and compared to a few significative experimental data sets in section 3.

1 REVIEW OF EXPERIMENTAL RESULTS

1.1 State-of-the-art review on crack tip analysis of strain-induced crystallizing rubber

Because it yields numerous material structure properties, Wide Angle X-ray Diffraction (Huneau 2011) has been the main tool used, among the numerous existing techniques, in order to characterize strain-induced crystallization in rubber. Very few studies considered SIC under fatigue loading conditions. In the 1970s, (Kawai 1975) successfully measured SIC in fatigue using a stroboscopic method in order to accumulate the weak diffracted intensity over hundreds of cycles. Beurrot (Beurrot 2012) overcame the difficulty of weak intensity using synchrotron radiation to reduce the exposure time to 1 s. It is also noted that only two papers investigated the crystallinity in the neighbourhood of a crack tip: (Lee 1987) measured the distribution of crystallinity along the propagation direction of a crack in both carbon black filled and unfilled NR, and (Trabelsi 2002) extended the WAXD measurements to the whole neighbourhood of the crack tip in unfilled NR. In both cases the measurements were performed at fixed stretch. More recently, Pierre Rublon (Rublon 2012) has presented an original experimental set-up developed to measure in real-time crystallinity around the crack tip in carbon black filled natural rubber during fatigue.

1.2 Reference experiment of Pierre Rublon

This test is done on a pure shear specimen described in figure 1 made of natural rubber filled with 50 p.h.r. of N347 carbon black. Once clamped on the homemade fatigue machine, the sample is first cycled for 300 cycles at a global stretch ratio of 1.92 and at a frequency of 2Hz in order to lower the residual stretch due to viscous and Mullins effects. After this preconditioning stage, a 20 mm-long cut is then made in one side of the relaxed sample. Next, a preliminary cyclic test which permits to transform the cutter incision into a fatigue crack is performed. During this transformation, the crack tip propagates by around 1mm from the cutter incision tip. This procedure is performed before each experiment at the same global stretch ration as that used during measurements. The simultaneous mechanical loading at different elongation ratios and WAXD mapping is then made following a particular procedure described in (Rublon 2012). Once the mapping is recorded, a post-processing analysis leads to the plot of 'iso-crystallinity' curves that gives the distribution of strain-induced crystallization around the crack tip for four global stretch ratios (figure 2). In these examples the minimal value of the crystallinity index is 0.1 due to post-processing difficulties. To finish, the author is well-aware of the characterization of the strain-induced crystallization behavior on an uncracked sample for the same conditions of speed and temperature (nominal stress and crystallinity versus stretch). But, this data is not available for public access.

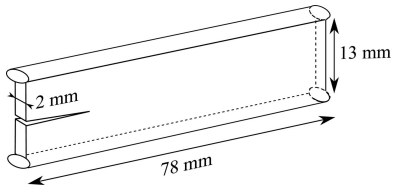

Figure 1: Pure shear specimen.

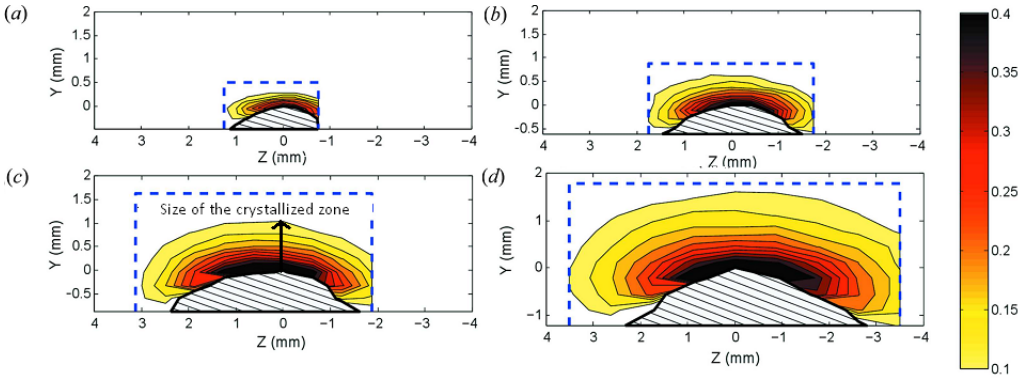

Figure 2: Index of crystallinity around a fatigue crack tip for different global stretch ratios: (a) 1.46, (b) 1.61, (c) 1.77 and (d) 1.92. Dotted lines show the measurement maps and the hatched zones represent the crack from Pierre Rublon

2 CONSTITUTIVE MODEL

In this section we propose a thermodynamically consistent way to construct a micro-sphere constitutive model of strain-induced crystallizing rubber, that is capable of reproducing the essential features described in (Guilie 2013a).

2.1 Free energy and internal variables for the 1D model

One must first model the purely amorphous part of the rubber. To achieve anisotropic 3D simulations, a natural choice for us is to use Miehe's popular model of the chain-tube system (Miehe 2004). In this model the energy of a representative chain in a given direction is given by the expression of a Langevin spring, for which the extensibility is finite. The interaction of the chain and the chain-network is rendered by adding a tube with a variable diameter which takes into account the confinement effect on the representative chain. The free energy for the chain assembly is obtained, by assuming chain and tube energies can be simply added and that all chains are in the same average

state, which gives the amorphous free energy

$$\psi_a(\lambda, T, \nu) = R_A T \left[F_\beta \left(\frac{\lambda}{\sqrt{N_{seg}}} \right) + U\nu \right], \tag{1}$$

with λ the chain elongation relative to his reference length, ν the relative shrinkage of the tube diameter, R_A the amorphous state stiffness, N_{seg} the number of segments in the representative chain, $F_\beta \left(\frac{\lambda}{\sqrt{N_{seg}}} \right)$ the free Langevin energy and U the tube modulus. When reaching the proper stress, crystallites appear in the amorphous medium. These crystallites introduce additional mechanisms observable at the constitutive scale: relaxation of the amorphous chains, network hardening due to morphology change and/or percolation of crystallites, crystal based increased elasticity observed at high deformations. Relaxation of the amorphous phase is taken into account by replacing the successive nucleations by the growth of a unique crystallite characterized by λ_χ. In consequence, the representative chain energy in the amorphous network will be replaced by the energy of the representative chain's amorphous part with local elongation $\lambda_l = \lambda - \lambda_\chi$. The mechanism of hardening seems to be somehow associated to the morphology of the crystallite. So, we propose to introduce a stored energy $g(\lambda_\chi)$

$$g(\lambda_\chi) = \begin{cases} g(0) = [0, \infty] \text{ for } \lambda_\chi < 0, \\ \mathrm{g}(\lambda_\chi) \text{ regular for } \lambda_\chi \in]0, \lambda_{\chi,sat}[, \\ g(\lambda_{\chi,sat}) = [\mathrm{g}(\lambda_{\chi,sat}), \infty]. \end{cases} \tag{2}$$

Next, the crystal based increased elasticity is simply modelled by a function $\psi_{el}(\lambda_\chi, \lambda) = R_B T F\left(\langle \lambda - \lambda^* \rangle_+\right)$ if $\lambda_\chi > 0$ with R_B the stiffness of the crystallizing medium and where the mechanism $F\left(\langle \lambda - \lambda^* \rangle_+\right)$ is activated from the value λ^* onwards. We finally add to the previous terms s_f the crystallite's formation entropy and h_f the crystallite's formation enthalpy. The following total free energy is finally proposed

$$\psi_{sc}(\lambda, \lambda_\chi, T, \nu) = R_A T \left[F_\beta \left(\frac{\lambda - \lambda_\chi}{\sqrt{N_{seg}}} \right) + U\nu \right] + g(\lambda_\chi) + \lambda_\chi (s_f T - h_f) + R_B T F\left(\langle \lambda - \lambda^* \rangle_+\right). \tag{3}$$

2.2 Thermodynamic force & Evolution laws

The free energy for a semi-crystalline system (3) isn't differentiable in λ_χ because of the way the g term is constructed. We must therefore make a distinction between the thermodynamic force during crystallization π^r_χ defined by the right derivative of ψ_{sc} in λ_χ for $\lambda_\chi \in [0, \lambda_{\chi,sat}[$ and λ_χ increasing from the thermodynamic force during fusion π^l_χ defined by the left derivative of ψ_{sc} in λ_χ for $\lambda_\chi \in]0, \lambda_{\chi,sat}]$ and λ_χ decreasing. Using the constitutive relations, Clausius-Duhem inequality reduces to

$$D = \pi^r_\chi \frac{\mathrm{d}\lambda_\chi}{\mathrm{d}t} \geq 0 \text{ if } \frac{\mathrm{d}\lambda_\chi}{\mathrm{d}t} \geq 0, D = \pi^l_\chi \frac{\mathrm{d}\lambda_\chi}{\mathrm{d}t} \geq 0 \text{ if } \frac{\mathrm{d}\lambda_\chi}{\mathrm{d}t} \leq 0. \tag{4}$$

We now need to introduce and identify a constitutive equation governing the evolution of λ_χ. We assume therefore that during evolution of this internal variable, Clausius-Duhem dissipation inequality is strict during crystallization, which is a natural assumption to make as the material's behaviour is dissipative on crystallization. During fusion the state is supposed to be a quasi-equilibrium, so there is no dissipation

$$\pi^l_\chi = 0 \text{ if } \frac{\mathrm{d}\lambda_\chi}{\mathrm{d}t} < 0. \tag{5}$$

The crystallization, which is late in comparison to equilibrium, is authorized only if the thermodynamic force is equal to a given threshold

$$\pi^r_\chi = Y(\lambda_{\chi,sat} - \lambda_\chi) \text{ if } \frac{\mathrm{d}\lambda_\chi}{\mathrm{d}t} > 0. \tag{6}$$

Here Y is a characteristic function of the material positive, increasing and such that $Y(0) = 0$ and $3\frac{R_A}{\sqrt{N_{seg}}} T_g + \frac{\partial^2 \mathrm{g}}{\partial \lambda_\chi^2} > -\frac{\mathrm{d}Y}{\mathrm{d}\lambda_\chi} \geq 0$. Temperature T_g is herein defined as the glass transition temperature below which the medium is completely crystallized and our model no longer applies. Altogether, this leads to an hardening plasticity like evolution law in crystallization and fusion and this evolution ensures the dissipation inequality.

2.3 Micro-sphere

This 1D model is then plugged into an affine micro-sphere approach. In this approach, each direction is free to have its own evolution, allows us to obtain an evolving anisotropy. To do that, we can consider the vector $\mathbf{R}$ defined in the reference configuration of the unit sphere which characterises the material direction under study and the isochoric part of the right Cauchy-Green tensor $\mathbf{C} = \mathbf{F}^\top\mathbf{F}$. Then, we propose to take λ and ν in each material direction as $\lambda = \sqrt{\mathbf{RCR}}, \nu = \sqrt{\mathbf{RC}^{-1}\mathbf{R}}$. Finally, the free energy (3) by direction is integrated in $\mathbf{R}$ over the unit sphere, and the contributions from representative polymer chains, oriented in all possible directions $\mathbf{R}$, are thus included. This constitutive law is implemented in the code Febio to do the following numerical tests.

3 VALIDATION

To reproduce the experiment presented in the section 1, we mesh a 3D pure shear sample (figure 1) and we introduce a 21 mm-long crack. In this sample, the mesh is adaptative with 84500 hybrid linear hexahedral elements. At the crack tip, the characteristic size of an element is 0.05 mm so as to have a minimum of 5 elements in the smallest crystallized zone ($\lambda = 1.46$). On the two faces of the sample, we applied a displacement so as to create a Mode I load for the crack like in the experiment. As the behavior law is known and already fixed, we then create a loading from $t = 0 \leftrightarrow \lambda = 1$ to $t = 1.0 \leftrightarrow \lambda = 1.92$. Then we compare one characteristics of our test with the experimental results, the size of the crystallized zone defined in figure 2 and computed in table 1. First, we observe that our results are 3D but the experimental results are 2D. In the experiment, measurements are summed up in the sample thickness because of the X-ray beam. To obtain something comparable, we also sum up the crystallinity index along the thickness. We begin to compare the size of the crystallized zone in table 1. We recall that the characteristic size of an element in front of the crack for simulation is 0.05 mm and 0.1 to 0.3 mm for experiment (Rublon 2012).

Elongation	d_p Model (mm)	d_p Experiment (mm)
1.46	0.31	0.29
1.61	0.53	0.85
1.77	0.90	1.04
1.92	1.62	1.62

Table 1: Comparison between model and experiment, size of the crystallized zone d_p.

4 CONCLUSION

The original experimental set-up used by (Rublon 2012) and the micro-sphere model for strain-induced crystallization permit to compare crystallinity distribution during a fatigue test. These firsts results are encouraging but to explain the good properties of NR in fatigue and more precisely its good resistance to fatigue crack growth in presence of SIC, one need a new fatigue life criterion taking into account this reinforcing mechanism.

REFERENCES

Beurrot, S. (2012). Cristallisation sous contrainte du caoutchouc naturel en fatigue et sous sollicitation multiaxiale. Thse de doctorat de l'Ecole Centrale de Nantes.

Guilie, J., Thien-Nga, L. & Le Tallec, P. (2013). Thermodynamic constitutive model for strain-induced crystallization, *submitted to Mech. of Materials.*

Huneau, B. (2011). Strain-induced crystallization of Natural Rubber: a review of Xray diffraction investigations, *Rubber Chem. Technol. 84*, 425-452.

Kawai, H. (1975). Dynamic X-ray diffraction technique for measuring rheo-optical properties of crystalline polymeric materials, *Rheol. Acta 14*, 27-47.

Lee, D. & Donovan, J. (1987). Microstructural Changes in the Crack Tip Region of Carbon-Black-Filled Natural Rubber, *Rubber Chem. Technol. 60*, 910-923.

Miehe, C., Goktepe, S. & Lulei, F. (2004). A micro-macro approach to rubber-like materials-Part I: the non-affine micro-sphere model of rubber elasticity. *Journ. of the Mech. and Phys. of Solids 52*, 2617–2660.

Rublon, P., Huneau, B., Saintier, N., Beurrot, S., Leygue, A., Verron, E. and al. (2012). In situ synchrotron wide-angle X-ray diffraction investigation of fatigue cracks in natural rubber, *J. of sync. rad. 20*, 0-0.

Trabelsi, S., Albouy, P.-A. & Rault, J. (2002). Stress-Induced Crystallization around a Crack Tip in Natural Rubber, *Macromolecules 35*, 10054-10061.